水下高压空气环境下 GMAW电弧特性试验

黄继强， 薛 龙， 吕 涛， 蒋力培
(北京石油化工学院 光机电装备技术北京市重点实验室，北京 102617)

黄继强

摘 要：采用高压试验舱模拟水下高压干式焊接环境，以压缩空气为气源进行加压，通过防燃爆试验验证在 0.1～0.7 MPa范围内，在 CO_2 和混合气（80% Ar+20% CO_2）作为保护气源的情况下，可以进行正常的 GMAW焊接过程. 在此基础上，通过试验研究了高压空气环境下 GMAW电弧特性，分别考察了环境压力、焊接电流、焊丝伸出长度和保护气种类及流量对焊接电弧特性的影响规律，并给出试验结果. 借助最小二乘法对试验数据进行拟合，得出了高压空气环境下 GMAW电弧电压的数学模型.

关键词：水下焊接；熔化极气体保护焊；电弧；高压焊接
中图分类号：TG403 文献标识码：A 文章编号：0253－360X(2010)12－0017－04

0 序 言

海底输油管线所处环境恶劣，易受到意外的机械外力作用和管道内部、外部腐蚀等影响而出现损坏并导致油气泄露[1,2]，这时需要对损坏管道进行快速维修，以保障海洋油气运输的安全和降低因油气泄露造成的海洋生态环境污染. 水下高压干式管道焊接修复技术被认为是快速、经济的维修方法之一[1－4]，但因过程复杂，国内研究滞后，未能得到推广应用.

水下高压干式焊接技术是采用焊接舱包裹住待修复工件，舱内充入高压气体以保证舱体内外压力基本平衡，焊接在完全干式环境之中进行. 与干式 GTAW相比，干式 GMAW适应性强，更适于自动化焊接，焊接效率高，对于作业环境危险、作业费用昂贵的水下修复而言非常有利. 高压干法水下焊接由于依靠高压气体将焊接区的水排开，其高压环境气体对焊接过程有明显的影响[4]. 目前国外常用的高压气体是氩气或氦气[5]，考虑到具体焊接成本等问题，该研究拟采用压缩空气作为高压气体. 为此，文中采用高压焊接试验舱模拟水下不同高压环境中进行系列焊接试验，研究水下高压空气环境下 GMAW的电弧特性，为采用 GMAW方法修复水下管道提供试验数据和技术依据，对提高国内水下管道修复焊接技术具有重要的现实意义.

收稿日期：2010－04－30
基金项目：国家 863高技术研究发展计划资助项目（2009AA04Z208）；北京石油化工学院青年科研基金资助重点项目（No. 08－03）

1 试验系统试验准备

1.1 试验系统

试验系统主要由高压焊接试验舱、焊接试验操作台架、高速摄像、远程监控系统和焊接电源等组成，试验系统原理如图 1所示. 其中高压焊接试验舱设计压力为 5.0 MPa，容积为 4 m^3. 空气压缩机用来提供高压空气至高压舱中以模拟水下高压焊接环境，空气压缩机出来的高压气体经过过滤后送入干燥器中，干燥器将高压气体的露点降至 －25 ℃以下，以避免高压潮湿空气对焊接过程的影响.

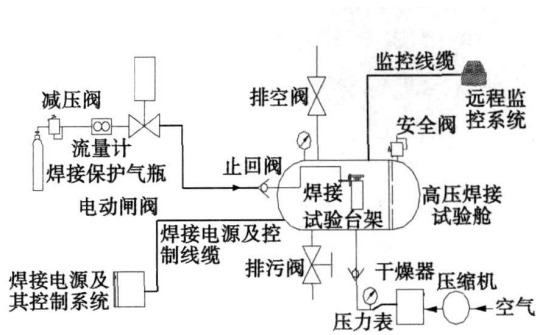

图 1 高压焊接试验装置原理图

Fig. 1 Schematic diagram of hyperbaric welding

焊接试验台架由工件旋转台、高速摄像、送丝机构、场景 CCD和照明系统等组成. 焊接试件放置在试验台架的旋转卡盘上，试验时，焊炬不动，试样随卡盘一起转动. 高速摄像机为 Mega Speed MS55K型，最高拍摄速度为 6 000帧/s 场景 CCD用于监

视焊接过程中坡口对中和观察焊缝成形情况. 高速摄像信号、场景 CCD信号传输至远处监控系统, 通过对远程监控系统的操作, 可以实时监控和调整焊接试验台架的工作状况. 焊接设备采用福尼斯 TPS3200 CMT焊接电源.

1.2 高压空气防燃爆试验

空气作为环境气体, 成本低而且随处可得, 只需要将其压缩至适当的压力即可使用. 但空气中的氧含量高, 在高压情况下存在安全问题. 为此, 采用空气作为加压介质, 焊接保护气分别为 CO_2 和混合气 (80% Ar+20% CO_2). 在 0.3, 0.5, 0.7 MPa 3个压力级别进行燃弧试验, 焊接电流为 150 A, 实时观察电弧燃烧情况. 试验结果表明, 在 0.1 ~0.7 MPa压力范围内, 随着压力增加, 电弧燃烧区域略有增强, 但未发生舱内其它地方明火燃烧或出现爆炸现象, 可以进行正常的焊接试验.

2 高压空气环境下的 GMAW电弧特性试验及结果分析

在上述高压焊接试验舱中进行不同空气环境压力下的 GMAW电弧特性试验, 焊接母材采用 ϕ168 mm×8 mm钢管, 材质为 API X65管线钢, 焊丝采用 JM-56, 焊丝直径为 1.0 mm, 两种保护气体分别为 CO_2 气体和 80% Ar+20% CO_2 混合气体. 在高压舱中分别进行了环境压力、焊接电流、焊丝伸出长度及保护气体等参数变化对电弧特性产生影响的试验研究.

2.1 环境压力的影响

在高压模拟试验舱中进行焊接试验, 保护气体流量为 20 L/min, 焊丝伸出长度为 10 mm, 环境压力采用 0.1, 0.3, 0.5 MPa 3种情况, 记录不同焊接电流时的电弧电压. 结果如图 2所示, 电弧电压均呈上升趋势, 随着电流的增加, 电弧电压逐步升高, 气压每升高 0.1 MPa, 电弧电压约升高 1 V左右 (还受到保护气体种类的影响). 从两种保护气体的特性曲线来看, 采用 CO_2 保护气体, 其电弧电压要略高于 80% Ar+20% CO_2 混合气体保护下的电弧电压.

以焊接电流为 100 A时的试验参数为例, 对不同环境压力下的电弧电压数据进行拟合, 可以分别得出两种保护气体下随环境压力 p与电弧电压 U 之间的关系曲线. 当焊接保护气体为 80% Ar+20% CO_2 时, 则

$$U=12.9+8.5p \quad (1)$$

当焊接保护气体为 CO_2 时, 则

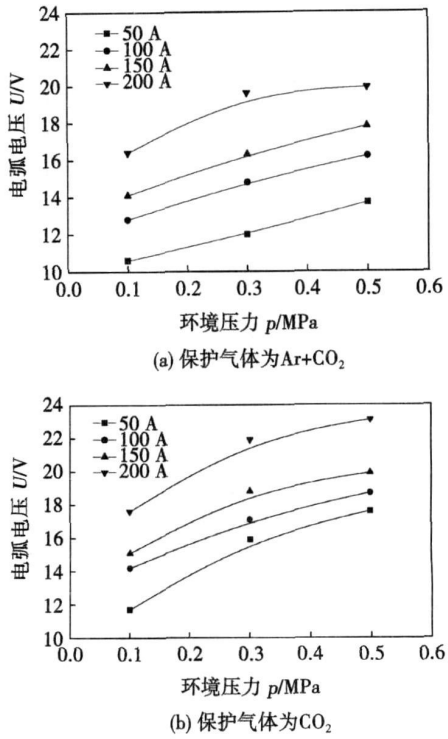

图 2 电弧电压随环境压力变化曲线

Fig. 2 Curves of relationship between arc voltage and pressure

$$U=14.4+11.2p \quad (2)$$

通过以上的试验来看, 随着环境压力的升高, 电弧电压具有上升特性, 所以, 要得到较为稳定的焊接过程, 当环境压力升高时, 应相应提高焊接电源的输出电压.

图 3给出了在焊接电流 I=200 A的情况下, 环境压力分别为 0.1, 0.3, 0.5 MPa电弧照片, 显然随着环境压力的增加, 焊接电弧更为集中, 电弧温度升高, 电弧烁亮区域增加.

2.2 焊接电流的影响

在环境压力变化的情况下, 不同的焊接电流对电弧电压存在比较明显的影响. 试验采用保护气体流量为 20 L/min, 焊丝伸出长度为 10 mm. 采用 50, 100, 150和 200 A焊接电流分别进行试焊, 记录下对应的电弧电压. 试验结果如图 4所示, 随着电流的增加, 电弧电压也呈线性上升趋势, 即电弧具有上升特性. 以 0.5 MPa环境压力下的试验数据为例, 在不同的保护气体下, 对试验数据进行拟合可分别得出焊接电流对电弧电压影响关系曲线. 当焊接保护气体为 80% Ar+ 20% CO_2 时, 则

$$U=12+0.038\,6I \quad (3)$$

焊接保护气体为 CO_2 时, 则

$$U=15.4+0.035\,4I \quad (4)$$

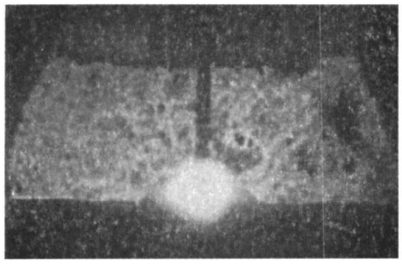

(a) 0.1 MPa

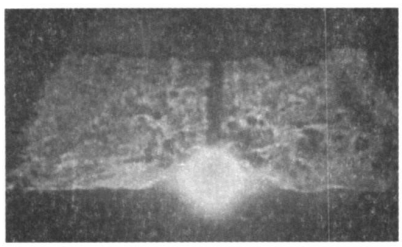

(b) 0.3 MPa

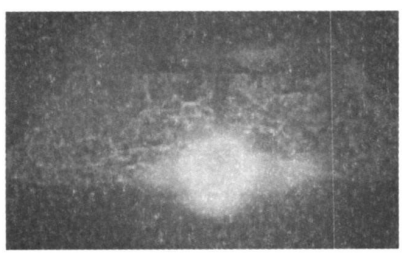

(c) 0.5 MPa

图3　不同环境压力下的电弧形貌

Fig. 3　Pictures of arc in different pressure

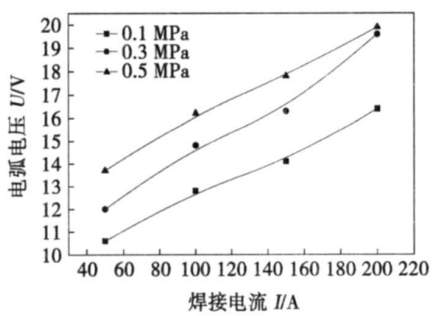

(a) 保护气体为Ar+CO_2

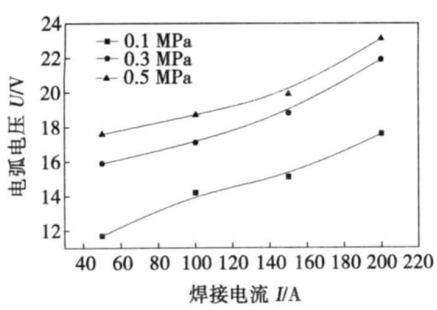

(b) 保护气体为CO_2

图4　电弧电压与焊接电流之间的关系曲线

Fig. 4　Curves of relationship between arc voltage and welding current

2.3　焊丝伸出长度的影响

在不同环境压力下，考察焊丝伸出长度对电弧电压的影响，试验采用保护气体流量为 20 L/min，焊接电流为 150 A，焊丝伸出长度 l 分别采用 10，15 和 20 mm 3种情况进行试验. 图 5给出了电弧电压与焊丝伸出长度之间的关系的试验结果，随着焊丝伸出长度的增加，电弧电压略有增加. 以 0.5 MPa 环境压力下试验数据为例，在不同保护气体下，分别对试验数据进行数据拟合得出焊丝伸出长度对电弧电压影响的关系曲线. 焊接保护气体为 80% Ar+20% CO_2 时，则

$$U=14.533+0.26l \tag{5}$$

焊接保护气体为 CO_2 时，则

$$U=17.6+0.24l \tag{6}$$

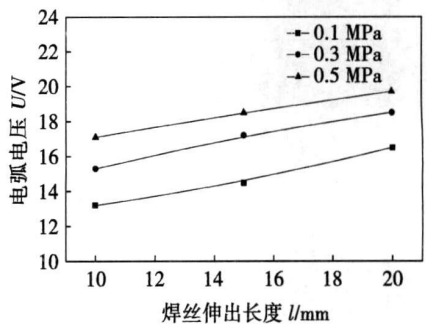

(a) 保护气体为Ar+CO_2

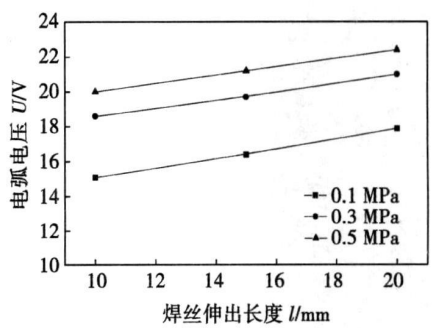

(b) 保护气体为CO_2

图 5　电弧电压与焊丝伸出长度之间的关系曲线

Fig. 5　Curves of relationship between arc voltage and stick-out

2.4　保护气体的影响

从前面的试验结果中可以明显看出，一般情况下，在其它焊接条件相同时，采用 CO_2 作为保护气体时，其电弧电压比采用 80% Ar+20% CO_2 混合气体保护下的电弧电压平均要高出 3～5 V，原因除了与保护气体的导热率和电离势差以外，CO_2 作为多原子分子，有较高的解离能，在高温下发生解离过程需要吸收大量的热能，这进一步增强了对电弧的冷却作用，造成电弧收缩效应明显，从而导致电弧电场

强度增加，电弧电压升高.

在不同环境压力下，还进行了保护气体流量变化对焊接过程的影响试验，试验采用焊接电流为 150 A，在不同的环境压力下分别采用 15、30、50 L/min 流量，观察焊接过程情况，并同时检测焊接电弧的特性，试验结果如图 6 所示，从试验的结果来看，在相同的环境压力下，随着气体流量的变化，电弧电压基本恒定. 也就是说，在上述的试验气体流量范围内，气体流量对电弧电压的影响不明显.

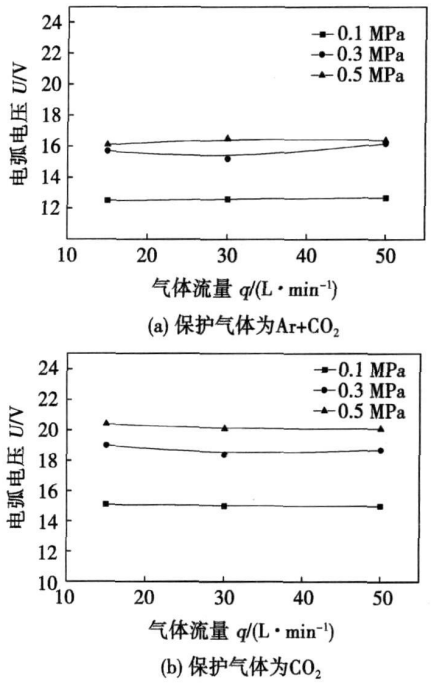

图 6 电弧电压与保护气体流量之间的关系曲线

Fig. 6 Curves of relationship between arc voltage and gas-flow

3 高压空气环境下的 GMAW 电弧电压的数学模型

综合前面的试验结果，电弧电压 U 与环境压力 P 之间呈线性关系，电弧电压 U 与焊接电流 I 呈线性关系，电弧电压 U 与焊丝伸出长度 l 也呈线性关系，且它们对电弧电压的影响相对独立，可以利用最小二乘原理进行多变量的数据拟合，从而分别获得电弧电压在不同保护气体下的数学模型. 当保护气体为 80% Ar+20% CO_2 时，则

$$U = 7.037 + 8.857P + 0.044I + 0.017l \quad (7)$$

当保护气体为 CO_2，则

$$U = 9.931 + 12.564P + 0.039I + 0.011l \quad (8)$$

上述模型将环境压力、焊接电流和焊丝伸出长度对电弧电压的影响统一起来，该模型的适用范围为环境压力 0.1 ~ 0.5 MPa，焊接电流为 50 ~ 200 A，焊丝伸出长度为 10 ~ 20 mm.

4 结 论

(1) 随环境压力、焊接电流、焊丝伸出长度增加，电弧电压增加，均导致电弧电特性呈上升趋势.

(2) 电弧特性受保护气体种类的影响明显，采用 CO_2 气体比 Ar+CO_2 混合气体的静态特性高；在满足正常的焊接情况下，气体流量对电弧特性影响不明显.

(3) 采用多变量线性拟合，得出了在 80% Ar+20% CO_2 混合气体和在 CO_2 气体保护下的数学模型. 为研究高压环境下 GMAW 焊接电弧电压变化规律及理论计算提供依据.

参考文献：

[1] Woodward N. Developments in diverless subsea welding[J]. Welding Journal, 2006(10): 35-39.

[2] Suga Y. On the arc welding under high pressure argon and helium atmosphere[C] // Welding Under Extreme Conditions. Oxford: Pergamon Press, 1989: 207-214.

[3] 蒋力培，王中辉，焦向东，等. 水下焊接高压空气环境下 GTAW 电弧特性[J]. 焊接学报，2007，28(6)：1-4.
Jiang Lipei, Wang Zhanghui, Jiao Xiangdong, et al. Characteristics of GTAW arc in underwater welding under high pressure air condition[J]. Transactions of the China Welding Institution, 2007, 28(6): 1-4.

[4] Hart P, Richardson IM, Nixon JH. The effects of pressure on electrical performance and weld bead geometry in high pressure GMA welding[C] // Welding in the World, 2001, 45(11/12): 31-37.

[5] Richardson IM, Nixon JH, Hart P, et al. Hyperbaric GMA welding to 2500 m water depth[C] // Proceedings of Joint International Conference ETC/OMAE, New Orleans, USA, 2000, 2000-2160.

作者简介：黄继强，男，1971 年出生，博士，副教授. 主要从事焊接机器人、特种焊接技术及电力电子等方面的研究工作. 发表论文 20 余篇.

Email: huangjiqiang@bipt.edu.cn

MAIN TOPICS, ABSTRACTS & KEY WORDS

fluently executed under the range of 0.1—0.7 MPa air pressure shielded by CO_2 and 80% Ar+20% CO_2 gases, which were tested by the igniting and exploding experiments using a hyperbaric cabin to simulate the underwater conditions. The arc characteristics of the GMAW were studied in hyperbaric conditions to discover the law of the arc affected by the environment pressure, the welding current, the stick-out, the gas type and the gas flow. The experiments results were also given, and a mathematical model under the high-pressure air condition was found by using the least square approximation method based on the experimental data.

Key words: underwater welding; gas metal arc welding; arc; hyperbaric welding

Analysis of vacuum projection welding by using finite element procedures YU Jiuyang, LU Xia, WANG Shixian, WANG Chenggang, YANG Xia (1. School of Mechanical Electrical Engineering, Wuhan Institute of Technology, Wuhan 430073, China; 2. School of Posts and Telecommunication Engineering, Wuhan Institute of Technology, 430073, China). p. 21—24

Abstract: Vacuum projection welding process was applied to MEMS package, which could improve yield rate and cut the cost. According to vacuum projection welding process, a thermal-electric-stress coupled field model was established, and the result of projection collapse and nugget growth process was discussed, which showed that the projection collapse occurred in the first half of part time, then metal around project was melt and final welding nugget was formed. Based on this analysis, the effect of projection tendon angle on welding quality was studied, and the result showed that fine welding quality was achieved when projection tendon angle is 60°. Simulation results agreed with the tensile test results after welding.

Key words: vacuum projection welding; thermal-electric-stress coupled field; projection tendon angle; finite element method

Coarse grained region microstructure and properties of high heat input welding DH36 steels CHAI Feng, SU Hang, YANG Caifu, LUO Xiaobing (Division for Structural Materials, Central Iron and Steel Research Institute, Beijing 100081, China). p. 25—28

Abstract: By using welding thermal simulation technology, coarse grained region microstructure and properties of high heat input welding DH36 steel were studied. The results show that low C, low Mn and low carbon equivalent with Ti treatment alloy design significantly improve the toughness of coarse grained region. The microstructures of coarse grained region change from thin lath M-A island to massive M-A island, and the amount of pro-eutectoid ferrite increases with the increasing of $t_{8/5}$. The island with size larger than 1 μm shows significantly effect on the toughness of coarse grained region. Decreasing the Mn content can promote the formation pro-eutectoid ferrite and inhibit the formation of M-A hard Phase at the same time, but excessive coarsening pro-eutectoid ferrite will decrease the low temperature toughness of coarse-grain HAZ obviously. The interaction of the M-A islands and pro-eutectoid ferrite affect the high heat input welding mechanical properties of DH36 steels.

Key words: high heat input welding; weld coarse grained region; pro-eutectoid ferrite; M-A island

Joint formation by twin-spot laser welding of 1420 aluminium-lithium alloy YANG Jing[1], LI Xiaoyan[1], GONG Shuili[1], CHEN Li[2], LI Qiaoyan[2] (1. College of Material Science and Engineering, Beijing University of Technology, Beijing 100022, China; 2. National Key Laboratory of Science and Technology on Power Beam Processes, Beijing Aeronautical Manufacturing Technology Research Institute, Beijing 100024, China). p. 29—32

Abstract: Based on the trial of twin-spot laser welding of 2 mm thick 1420 Al-Li alloy, the effect of laser welding parameters including laser power, welding speed, defocusing distance and twin-spot adjust parameters including focus spacing, focus orientation, intensity distribution of the foci on the formation of the joints was studied. The characteristics of weld formation in single-spot and twin-spot welding were compared and analyzed. The results indicated that the process window in twin-spot laser welding was narrower than in single spot laser welding, but the weld quality was improved prominently. The effect of focus spacing on the weld formation was related to intensity distribution of the foci, which had an essential influence on the welding result. In order to get a higher penetration and failure free seams, a 40% to 60% and a 60% to 40% distribution were better. Furthermore, the focus orientation had another slight impact on the welding result.

Key words: aluminium-lithium alloy; twin spots; laser welding; formation

Analysis of temperature field for TIG welding fine grain titanium alloy thin sheet ZHOU Shuiliang, TAO Jun, DU Yuxiao, GUO Delun (Aeronautical Key Laboratory for Aviation Joining Technology, Beijing Aeronautical Manufacturing Technology Research Institute, Beijing 100024, China). p. 33—36

Abstract: The temperature field for the conventional TIG welding of fine grain titanium alloy Ti-6Al-4V with different grain sizes is studied by numerical and experimental methods. The results show that the temperature field patterns and the temperature developing histories of fine grain Ti-6Al-4V alloy with different grain sizes are similar. But because of the refinement of base material grain size and the increment of grain boundaries, thermal conductivity and specific heat are both reduced, and the value of specific heat reduced is larger than that of thermal conductivity. So the heat conduction abilities of finer grain titanium alloy are weakened, the isothermal range of fine grained titanium alloys is larger than that of coarse grained titanium alloys, and the further the distances to central line of weld is, the more visible the difference is. The peak temperature of points with same distances to central line in fine grained titanium alloy is higher than that in coarse grained titanium alloy.

Key words: fine grain titanium alloy; temperature field; thermal conductivity; specific heat

Detailed effect of spot welding process on spot quality of high-strength aluminum alloy used in astronavigation